1 Variation in genome content and predatory phenotypes between *Bdellovibrio* sp. NC01 isolated

2 from soil and *B. bacteriovorus* type strain HD100

3 Laura E. Williams[a]#, Nicole Cullen[a], Joseph A. DeGiorgis[a,b], Karla J. Martinez[a], Justina

4 Mellone[a], Molly Oser[a]

5 [a]Department of Biology, Providence College, Providence, RI, USA

6 [b]Cellular Dynamics Program, Marine Biological Laboratory, Woods Hole, MA, USA

7 Running title: Genome and phenotype of *Bdellovibrio* from soil

8 #Corresponding author: Laura E. Williams, lwillia7@providence.edu

9

Abstract

The range of naturally occurring variation in the ability of *Bdellovibrio* strains to attack and kill Gram-negative bacteria is not well understood. Defining phenotypic and associated genotypic variation among *Bdellovibrio* will clarify how divergent lineages within this genus impact microbial communities and will inform development of predatory bacteria as biocontrol agents to combat bacterial infections. We isolated *Bdellovibrio* sp. NC01 from soil and compared its genome and predatory phenotypes to *B. bacteriovorus* type strain HD100. Based on analysis of 16S rRNA gene sequences and average amino acid identity, NC01 belongs to a different species than HD100. Genome-wide comparisons and individual gene analyses indicated that eight NC01 genome regions were likely acquired by horizontal gene transfer (HGT), further supporting an important role for HGT in *Bdellovibrio* genome evolution. Within these regions, multiple protein-coding sequences were assigned predicted functions related to transcriptional regulation and transport; however, most were annotated as hypothetical proteins. Compared to HD100, NC01 has a limited prey range and kills *E. coli* ML35 less efficiently. Whereas HD100 drastically reduces the ML35 population and then maintains low prey population density, NC01 causes a smaller reduction in ML35, after which the prey population recovers, accompanied by a decrease in NC01. In addition, NC01 forms turbid plaques on lawns of ML35, in contrast to clear plaques formed by HD100. Characterizing variation in interactions between *Bdellovibrio* and Gram-negative bacteria, such as observed with NC01 and HD100, is important for understanding the ecological significance of predatory bacteria and evaluating their effectiveness in clinical applications.

33 **Importance**

34 *Bdellovibrio* attack and kill Gram-negative bacteria; however, not all *Bdellovibrio* strains
35 are equally efficient at killing the same Gram-negative bacteria. Defining how *Bdellovibrio* vary
36 in predatory phenotypes and how this phenotypic variation relates to differences in genotype is
37 important for understanding the ecological significance of predatory bacteria and evaluating their
38 effectiveness in biocontrol of bacterial infections. We determined variation in genome content
39 and predatory phenotypes, including prey range and predation efficiency, between *Bdellovibrio*
40 sp. NC01 isolated from soil and *B. bacteriovorus* type strain HD100. NC01 is phylogenetically
41 divergent from HD100, with eight regions of unique gene content likely acquired by horizontal
42 gene transfer. Compared to HD100, the prey range of NC01 is limited, and it was less efficient at
43 killing a strain of *E. coli*. These differences may have important implications for how each strain
44 impacts microbial communities in different environments and for the effectiveness of each in
45 clinical applications.

46

47 **Introduction**

48 Since their discovery in the early 1960s, predatory bacteria have been isolated from a
49 wide range of terrestrial and aquatic environments, including some with extreme conditions such
50 as high temperature or salinity (1). The impact of predatory bacteria in these environments is not
51 fully known, but initial studies indicate they may play an important role in shaping microbial
52 communities (2–4). In addition, their ability to attack and kill Gram-negative bacterial pathogens
53 has generated interest in developing predatory bacteria as biocontrol agents to combat drug-
54 resistant infections (5–7). Given their potential ecological significance and possible clinical
55 applications, it is important to define phenotypic and genotypic variation among predatory

56 bacteria. In particular, variation in the outcomes of interactions between different strains of
57 predatory bacteria and prey will determine the impact of bacterial predation in microbial
58 communities, and variation in genome content among predatory bacteria strains may directly
59 affect those outcomes. To broaden our understanding of variation in predatory bacteria, we
60 isolated, assayed and sequenced a *Bdellovibrio* strain from soil and compared its predatory
61 phenotypes and genome content to other sequenced *Bdellovibrio*.

62 Among the different genera of predatory bacteria, *Bdellovibrio* is the most well-studied.
63 Currently, this genus includes two species that differ in their predation strategy. *B. bacteriovorus*
64 invades the periplasm of Gram-negative prey cells (8), whereas *B. exovorus* attaches to the
65 outside of prey cells but does not enter the cell itself (9). Here, we focus on intraperiplasmic
66 *Bdellovibrio*. This lifecycle includes two main phases: the attack phase and the growth phase
67 (10). During the attack phase, small, highly motile *Bdellovibrio* cells seek out and attach to
68 Gram-negative prey bacteria. *Bdellovibrio* then gains access to the prey periplasm by using lytic
69 enzymes to open a small hole in the prey outer membrane and cell wall (11). After *Bdellovibrio*
70 moves into the prey periplasm, it uses peptidoglycan-modifying enzymes to reseal and reshape
71 the prey cell wall, resulting in formation of a rounded structure called a bdelloplast (12). Within
72 the bdelloplast, *Bdellovibrio* initiates the growth phase, during which it secretes lytic enzymes
73 into the prey cytoplasm. Using digested prey cell contents as nutrients, *Bdellovibrio* grows into a
74 single long filament within the prey periplasm, eventually dividing into multiple progeny, which
75 lyse the bdelloplast and emerge as new attack phase cells.

76 By invading and lysing Gram-negative bacteria, some strains of *Bdellovibrio* can reduce
77 prey populations by up to 8 log units over 48 hours *in vitro* (6, 13). However, not all *Bdellovibrio*
78 strains are equally effective at killing the same Gram-negative species. Researchers have

79 observed variation among *Bdellovibrio* strains in which Gram-negative bacteria are susceptible
80 to predation (14) and in how quickly and to what extent a population of Gram-negative prey is
81 reduced (13, 15). These predatory phenotypes, referred to as prey range and predation efficiency,
82 are clearly important in determining the outcomes of interactions between *Bdellovibrio* strains
83 and Gram-negative bacteria; however, the extent of naturally occurring variation in these
84 phenotypes and the underlying mechanisms governing them are not well understood. Defining
85 how predatory phenotypes differ among *Bdellovibrio* will contribute to our understanding of the
86 impact of predatory bacteria on microbial communities in different environments and inform
87 their application in biocontrol of bacterial pathogens.

88 Here, we describe isolation of *Bdellovibrio* sp. NC01 from soil and compare its genome
89 and predatory phenotypes to other *Bdellovibrio*, focusing primarily on the *B. bacteriovorus* type
90 strain HD100. The intraperiplasmic predator HD100 was the first *Bdellovibrio* strain sequenced
91 (16), and multiple studies have dissected some of the molecular mechanisms governing predation
92 in this strain (17). To investigate variation in genome content, we compared the genome of NC01
93 to that of HD100 and *B. bacteriovorus* W, which is phylogenetically divergent from HD100 (18,
94 19). To define variation in predatory phenotypes between NC01 and HD100, we determined prey
95 range by testing each strain against a panel of Gram-negative bacteria, and we measured
96 predation efficiency by quantifying viable *E. coli* ML35 during co-culture with each strain.

97 **Results**

98 **Bioswale soil harbors predatory bacteria belonging to *Bdellovibrio***

99 Using Gram-negative soil bacteria isolated from a residential area as prey, we obtained a
100 pure isolate of predatory bacteria from a sample of soil collected at a bioswale on the Providence
101 College campus. The bioswale is a manmade landscape feature designed to collect and filter

102 stormwater runoff from nearby buildings. We designated the bioswale soil isolate as NC01.
103 Using 1000x phase-contrast microscopy of lysates combining NC01 and Gram-negative prey, we
104 observed small, fast-moving attack phase NC01 cells that attached to prey cells (Figure 1a). We
105 also observed rounded structures characteristic of bdelloplasts, suggesting that NC01 uses a cell
106 invasion strategy similar to *Bdellovibrio bacteriovorus*. Negative stain electron microscopy
107 showed that NC01 attack phase cells have a comma-shaped morphology with a single polar
108 flagellum (Figure 1b).

109 To classify NC01, we constructed a phylogeny of 16S rRNA gene sequences from this
110 isolate and all *Bacteriovorax*, *Bdellovibrio* and *Halobacteriovorax* strains with complete
111 genomes available in GenBank (Figure 2). In this phylogeny, NC01 clearly clusters with other
112 *Bdellovibrio*. Pairwise alignment of 16S rRNA gene sequences from NC01 and *Bdellovibrio*
113 *bacteriovorus* HD100, which is the type strain of the species, showed 97% similarity across
114 1,516 nucleotides. This value is above the 95% similarity cutoff typically used to define bacterial
115 genera (20), which supports classifying NC01 as *Bdellovibrio*. However, it is below the 98.7%
116 similarity cutoff typically used to define species (21), which suggests that NC01 should not be
117 classified as *bacteriovorus*.

118 To explore this further, we compared the average amino acid identity (AAI) of
119 *Bdellovibrio* strains NC01, W, HD100 and 109J (Table 1). HD100 and 109J, which are both
120 classified as *B. bacteriovorus*, cluster in a well-supported clade in the 16S rRNA phylogeny, and
121 their protein sequences are highly similar (average AAI 99.2%). However, NC01 protein
122 sequences are <70% similar on average to HD100 and 109J protein sequences, supporting the
123 conclusion that NC01 belongs to a different species than these two strains. NC01 protein
124 sequences are even less similar on average to those of strain W, suggesting that NC01 does not

125 belong to the same species as this strain. Based on these analyses, we chose not to designate a
126 species for NC01, and we refer to this isolate as *Bdellovibrio* sp. NC01.

127 **Comparative genomics identifies eight regions of unique gene content possibly acquired by**
128 ***Bdellovibrio* sp. NC01 via horizontal gene transfer**

129 Based on the 16S rRNA gene phylogeny and average AAI comparisons, we chose *B.*
130 *bacteriovorus* HD100 and *B. bacteriovorus* W to represent phylogenetic diversity and genome
131 variation among sequenced *Bdellovibrio* for comparative genomics. The genome of *Bdellovibrio*
132 sp. NC01 is larger than that of both HD100 and W (Table 2). The GC content of the NC01
133 genome is lower than that of HD100, but slightly higher than that of W. Using the BLAST Ring
134 Image Generator (BRIG), we conducted pairwise comparisons of NC01 to HD100 and W based
135 on nucleotide sequence alignments with BLASTN. This analysis identified eight NC01 genome
136 regions of at least 15,000 nucleotides in which no alignments of >200 nucleotides and e-value
137 <0.1 to HD100 or W were reported. These eight regions, which may represent unique NC01 gene
138 content, are marked on Figure 3. The plot of GC content shows that four of the eight regions
139 (regions 1, 4, 5, and 7) encompass substantial decreases in GC content compared to the typical
140 variation along the genome. Such deviation in GC content may be an indicator of horizontal gene
141 transfer (HGT) (22).

142 To assess whether the genes encoded in these eight NC01 genome regions are present but
143 divergent in HD100 and W, we used TBLASTN to compare NC01 amino acid sequences
144 annotated in each region by RAST to the HD100 and W genomes translated into all six reading
145 frames. RAST annotated 11 to 50 protein-coding sequences within each of the eight NC01
146 genome regions. By searching for these sequences along the entire HD100 and W genomes, this
147 analysis detects similar protein-coding sequences even if the genes have undergone

148 rearrangement. For the majority of the protein-coding sequences in each of the eight NC01
149 regions, TBLASTN did not produce any alignments to HD100 or W with >70% query coverage.
150 For those protein-coding sequences that did align to HD100 and/or W with >70% query coverage,
151 identity was low (<40%) for most of the sequences. Less than five protein-coding sequences in
152 each region aligned to HD100 or W at >70% coverage and >40% identity. This suggests that the
153 protein-coding sequences in the eight NC01 genome regions are missing from HD100 and W,
154 instead of divergent.

155 In addition to comparisons against HD100 and W, we also used BLASTP to align amino
156 acid sequences annotated in each region by RAST against the non-redundant GenBank database.
157 For each sequence, we examined the top 250 alignments for any sequences classified as
158 *Bdellovibrio*. This analysis expands the search space beyond complete *Bdellovibrio* genomes to
159 any deposited sequences that were denoted by the submitters as *Bdellovibrio*. In two of the
160 regions (regions 1 and 4), only one-third of amino acid sequences aligned to *Bdellovibrio*
161 sequences. In every other region except region 8, 52-64% of the amino acid sequences aligned to
162 *Bdellovibrio* sequences. In region 8, three-fourths of the amino acid sequences aligned to
163 *Bdellovibrio* sequences. These results suggest that most of the protein-coding sequences in
164 regions 1 and 4 may be unique to *Bdellovibrio* sp. NC01, because they do not align to other
165 *Bdellovibrio* sequences in the database. In the other regions, the larger proportion of shared gene
166 content between NC01 and *Bdellovibrio* in the database may be the result of HGT events that
167 occurred before the divergence of NC01 and these strains.

168 The hypothesis that the eight NC01 genome regions were acquired by horizontal gene
169 transfer is also supported by predicted functions of the protein-coding sequences encoded within
170 the regions. RAST annotation identified functions related to mobile elements in five of the eight

171 regions. These include phage tail fibers (regions 1, 5 and 6), site-specific recombinases or
172 integrases (regions 1, 4, and 7), a phage-related DNA primase (region 4), and a plasmid
173 conjugative transfer protein (region 7). In addition, Prophinder analysis of the complete NC01
174 genome identified a portion of region 5 (1,632,099 – 1,632,833) as a possible prophage. Three
175 regions (regions 2, 3 and 8) did not encode any obvious mobile element functions.

176 Apart from mobile element-related genes, most of the protein-coding sequences in the
177 eight NC01 genome regions are annotated as hypothetical proteins, therefore it is unclear what
178 functional capacities may have been gained by *Bdellovibrio* sp. NC01 via HGT and whether
179 those functions impact predation. Some of the genes were annotated with predicted functions,
180 which enabled us to assess gene content in the eight regions in terms of broad functional
181 categories. Four of the eight regions (regions 1, 3, 6 and 8) encode predicted functions related to
182 transcriptional regulation, and five regions (regions 1, 3, 5, 6, and 7) encode predicted functions
183 related to transport. Regarding enzymatic activity, region 6 encodes a predicted cell wall
184 endopeptidase, which is interesting given *Bdellovibrio*'s interactions with the Gram-negative
185 prey cell wall during its life cycle.

186 ***Bdellovibrio* sp. NC01 has a limited prey range compared to HD100 and is less efficient at**
187 **killing *E. coli* ML35**

188 To assess variation in predatory phenotypes between *Bdellovibrio* sp. NC01 and *B.*
189 *bacteriovorus* HD100, we assayed prey range and predation efficiency. To determine prey range,
190 we tested NC01 and HD100 against a panel of eight Gram-negative bacteria isolated from
191 different environments, including a freshwater stream and soil from a residential area (Table 3).
192 Plaque formation on a bacterial lawn indicates that the predatory isolate is able to attack and lyse
193 that particular Gram-negative prey strain. NC01 formed plaques on lawns of five of the eight

194 prey strains tested, whereas HD100 formed plaques on lawns of all eight prey strains. NC01 was
195 not able to attack and lyse two prey strains belonging to *Acinetobacter* and *Raoultella* that were
196 isolated from a freshwater stream. In addition, although NC01 formed plaques on *E. coli* ML35,
197 it did not attack and lyse *E. coli* 0057.

198 To measure predation efficiency, we quantified viable *E. coli* ML35 at different time
199 points over 72 hours of co-culture with NC01 or HD100 (Figure 4). In the absence of predatory
200 bacteria, we did not observe any reduction in viable *E. coli* ML35, demonstrating that co-culture
201 conditions do not adversely affect the ML35 population. After 6 hours of co-culture, NC01 did
202 not appreciably reduce viable *E. coli* ML35 compared to the control, whereas HD100 reduced
203 viable ML35 by approximately 1 log unit. After 24 hours of co-culture, there was a substantial
204 difference in the impact of NC01 and HD100 on the *E. coli* population. NC01 reduced viable
205 ML35 by approximately 3 log units compared to the control, whereas HD100 reduced viable
206 ML35 by 6 log units. Over the next 48 hours, HD100 continued to restrict the viable ML35
207 population, but the population recovered in co-cultures with NC01, increasing by 2 log units.

208 For two of the assay replicates, we quantified NC01 and HD100 after 72 hours of co-
209 culture to determine if recovery of the ML35 population is associated with changes in predatory
210 bacteria population density. Based on direct cell counts used to establish co-cultures, both NC01
211 and HD100 populations were ~10^8 cells/ml at the beginning of the assay (NC01: 3.8 x 10^8
212 cells/ml and 7.8 x 10^8 cells/ml, HD100: 4.1 x 10^8 cells/ml and 9.8 x 10^8 cells/ml). After 72 hours
213 of co-culture with *E. coli* ML35, plaque counts showed a small decrease in the HD100
214 population (1.5 x 10^8 pfu/ml and 4.5 x 10^8 pfu/ml), whereas the NC01 population decreased
215 substantially (2.3 x 10^5 pfu/ml and 7.5 x 10^6 pfu/ml). When compared in validation tests, direct
216 cell counts and plaque counts yielded comparable results, therefore the observed decrease in

217 NC01 population is not due to a difference in methods for determining predator population
218 density. These data demonstrate that for both NC01 and HD100, active predatory bacteria are
219 present after 72 hours of co-culture with *E. coli* ML35, but, in contrast to HD100, the NC01
220 population density decreases by at least two orders of magnitude over the course of the predation
221 efficiency assay.

222 **Plaques formed by *Bdellovibrio* sp. NC01 on *E. coli* ML35 prey lawns are not as clear as**
223 **those formed by HD100**

224 In addition to quantitative differences in the ability of *Bdellovibrio* sp. NC01 and *B.*
225 *bacteriovorus* HD100 to kill *E. coli* ML35, we also observed qualitative differences in the
226 appearance of plaques formed by each strain on lawns of ML35 (Figure 5). In contrast to HD100,
227 which forms completely clear, regular plaques, NC01 forms plaques of a similar size, but with
228 incomplete clearance of the prey lawn within the plaques. Some NC01 plaques remain
229 completely turbid over eight days of incubation, whereas others retain a turbid center but begin
230 to clear on the edges of the plaque.

231 **Discussion**

232 We isolated *Bdellovibrio* from soil collected at a manmade landscape feature designed for
233 stormwater management on a college campus. By comparing 16S rRNA gene sequences and
234 analyzing average amino acid identity (AAI) among multiple sequenced *Bdellovibrio*, we
235 determined that the *Bdellovibrio* isolate was sufficiently divergent from *B. bacteriovorus* type
236 strain HD100 and other *B. bacteriovorus* strains that it should be classified as a different species.
237 The only other species currently described within *Bdellovibrio* is *exovorus*; however, this species
238 uses an epibiotic predation strategy that differs from the cell invasion strategy observed by
239 microscopy for the soil *Bdellovibrio* isolate described here. Pending further characterization, we

240 designated the isolate as *Bdellovibrio* sp. NC01. Our analysis of 16S rRNA sequences and
241 average AAI also suggests that *Bdellovibrio* strain W is divergent enough from both HD100 and
242 NC01 to warrant its own species designation. This is consistent with the reported ability of W to
243 form a resting stage called a "bdellocyst", which has not been observed for any other
244 *Bdellovibrio* so far (18, 23).

245 Because *Bdellovibrio* sp. NC01 is phylogenetically divergent from HD100 and other
246 *Bdellovibrio* with sequenced genomes, this isolate provides a valuable opportunity to assess
247 variation in genome content and predatory phenotypes among *Bdellovibrio*. Genome-wide
248 comparisons of NC01 to HD100 and W using BLASTN identified eight regions of unique gene
249 content along the NC01 genome, and TBLASTN confirmed that the protein-coding sequences
250 within these regions are missing from the genomes of HD100 and W. Multiple lines of evidence
251 support the hypothesis that these eight regions were acquired by *Bdellovibrio* sp. NC01 via
252 horizontal gene transfer. Four of the regions have substantially lower GC content than the
253 genome average, which may indicate horizontal acquisition from a bacterial genome with a
254 lower average GC content than that of NC01 (22). Five of the regions encode genes with
255 predicted functions related to mobile elements such as phage and plasmids, and one of these
256 regions was identified as a possible prophage by phage finding sequence analysis software.

257 Alignment by BLASTP of amino acid sequences encoded within two of the eight regions
258 against the GenBank database suggested that these two regions may have been acquired recently
259 by *Bdellovibrio* sp. NC01, because most of the sequences did not align to *Bdellovibrio* sequences
260 (complete or partial) in the database. This indicates that, given the current representation of
261 *Bdellovibrio* in the database, gene content in these two regions is mostly unique to NC01. For the
262 other six regions, the majority of amino acid sequences encoded in these regions aligned to

263 *Bdellovibrio* sequences in the database. This suggests that these *Bdellovibrio* strains may be
264 closely related to NC01, and the HGT events corresponding to acquisition of these six regions
265 occurred in the ancestral lineage before NC01 diverged from these strains. Addition of more
266 complete *Bdellovibrio* genomes to the database will improve our ability to reconstruct
267 evolutionary events such as horizontal gene transfer.

268 The analysis of *Bdellovibrio* sp. NC01 gene content reported here further illustrates the
269 role of horizontal gene transfer as an important force in predatory bacteria genome evolution.
270 Comparative genomics has yielded evidence of both ancient and recent HGT in *Bdellovibrio* and
271 in the saltwater-adapted predatory genus *Halobacteriovorax* (24–27). However, lack of
272 functional annotation of many *Bdellovibrio* protein-coding sequences prevents a thorough
273 assessment of how HGT events impact predatory phenotypes. Within the eight NC01 genome
274 regions likely acquired via HGT, many of the protein-coding sequences are annotated as
275 hypothetical proteins, which provides no insight into their function and their potential roles in the
276 predatory life cycle. To fully understand how *Bdellovibrio* genome variation relates to variation
277 in predatory phenotypes, it is essential to assign functions to protein-coding genes.

278 In addition to genome comparisons, we also compared predatory phenotypes between
279 *Bdellovibrio* sp. NC01 and *B. bacteriovorus* type strain HD100. Based on plaque formation on
280 lawns of eight different Gram-negative bacteria, NC01 has a more restricted prey range than
281 HD100. In particular, HD100 was able to attack and kill both tested strains of *E. coli*, whereas
282 NC01 was only able to attack and kill *E. coli* ML35. Other researchers have also observed that a
283 particular *Bdellovibrio* strain may vary in its ability to kill different members of the same species
284 (14, 28); however, the mechanisms governing these outcomes are not known. By demonstrating
285 that strain-level variation within a Gram-negative species determines susceptibility to predation,

286 these data have potentially important implications for developing predatory bacteria as
287 biocontrol agents in the treatment of bacterial infections. If a *Bdellovibrio* isolate attacks and
288 kills one representative of a Gram-negative species, it does not guarantee that the isolate will
289 attack and kill other strains within the species. Further work to define the molecular mechanisms
290 underlying variation in prey range may enable prediction of whether a Gram-negative strain will
291 be susceptible to predation by a particular *Bdellovibrio* strain.

292 Although both NC01 and HD100 can attack and kill *E. coli* ML35, predation by HD100
293 causes a greater reduction in the ML35 population after 24 hours *in vitro* compared to predation
294 by NC01. HD100 then maintains a low ML35 population density, although it does not
295 completely eliminate viable ML35. By contrast, in co-cultures of NC01 and ML35, the ML35
296 population recovers after 24 hours, whereas the NC01 population decreases. This is likely not the
297 result of general predator-prey dynamics, such as an increase in search time due to reduced
298 ML35 numbers, because we did not observe ML35 population recovery in co-cultures with
299 HD100. Other researchers have observed similar prey population recovery (29, 30), and
300 Shemesh and Jurkevitch demonstrated that recovery of *Erwinia carotovora* in co-cultures with
301 *Bdellovibrio* isolated from soil was due to development of phenotypic resistance to predation. It
302 is possible that *E. coli* ML35 uses a similar mechanism to develop resistance to predation by
303 *Bdellovibrio* sp. NC01, but this mechanism is either not expressed or not successful in co-
304 cultures with *B. bacteriovorus* HD100. Further work will test this hypothesis and define the
305 molecular mechanisms governing ML35 population recovery.

306 Differences in predation efficiency between NC01 and HD100 on *E. coli* ML35 may also
307 be related to variation in plaque phenotype. Plaques formed by NC01 on lawns of ML35 are
308 turbid, whereas plaques formed by HD100 are completely clear. Turbid plaques have been

309 reported as a characteristic of prey-independent mutants of *Bdellovibrio*; however, these plaques
310 are typically smaller than those formed by the wild-type strain and sometimes have a small
311 colony of host-independent *Bdellovibrio* at their center (31, 32). Neither of these features were
312 observed when comparing NC01 and HD100 plaques, suggesting that the NC01 plaque
313 phenotype is not the result of prey-independent growth. Turbid plaques formed by NC01 may
314 arise from incomplete lysis of *E. coli* ML35 cells. If prey cells are successfully invaded but not
315 lysed, *Bdellovibrio* progeny will be trapped, which would explain the incomplete clearance of
316 the prey lawn and the decrease in the NC01 population observed during predation efficiency
317 assays. Further work will test this hypothesis.

318 Overall, comparisons between *Bdellovibrio* sp. NC01 and *B. bacteriovorus* HD100
319 revealed variation in predation phenotypes that may have important implications for the
320 ecological impact of each of these strains and their effectiveness in clinical applications. The
321 molecular mechanisms governing phenotypes such as prey range and predation efficiency are not
322 known. Comparative genomics can generate hypotheses linking gene content differences to
323 observed phenotype differences, but the lack of functional annotation for many protein-coding
324 genes complicates this effort. It is also likely that the outcomes of interactions between predatory
325 bacteria and prey, such as whether or not two different *Bdellovibrio* can kill the same Gram-
326 negative strain, are dependent upon mechanisms specific to the *Bdellovibrio* strain and
327 mechanisms specific to the prey strain. Defining these mechanisms is key for understanding
328 variation in predatory phenotypes among divergent *Bdellovibrio*.

329 **Materials and Methods**

330 **Isolation and classification of environmental bacteria for use as prey**

331 We isolated bacteria from an urban freshwater stream in Providence, RI (41.835, -
332 71.44299) and from soil in a residential area of Massachusetts (42.0877, -71.2309) for use as
333 prey. We also obtained *E. coli* ML35 from Mark Martin (University of Puget Sound, Puget
334 Sound, WA) and *Escherichia* 0057 from Brett Pellock (Providence College, Providence, RI).
335 To classify these isolates, we sequenced the 16S rRNA gene following a previously
336 described procedure (24). Briefly, we used primers 63F (33) and 1378R (34) to amplify the 16S
337 rRNA gene. Sanger sequencing of purified PCR products was performed by GeneWiz (South
338 Plainfield, NJ) using the same primers. We trimmed and assembled reads using
339 Phred/Phrap/Consed (35–37), then classified the assembled 16S rRNA gene sequences using
340 BLAST (38), the SILVA Incremental Aligner (39) and the Ribosomal Database Project classifier
341 (40). Supplementary Table 1 shows the full classification results. The RDP classifier and the
342 SILVA Incremental Aligner classify sequences to the genus level, but not the species level;
343 therefore, species names are not provided for these isolates.
344 **Isolation and classification of *Bdellovibrio* sp. NC01 from bioswale soil**
345 In September 2015, we collected 50 g of soil from a bioswale on the Providence College
346 campus (41.84277, -71.43944). We combined the soil sample with 500 ml of sterile HM buffer
347 (25 mM HEPES adjusted to pH 7.4 and supplemented with 3 mM calcium chloride dihydrate and
348 2 mM magnesium chloride hexahydrate). We then filtered this mixture through sterile
349 cheesecloth into a sterile container to remove large particulate matter. We vortexed the filtrate to
350 release bacterial cells from the small particles of soil that passed through the cheesecloth. To
351 pellet the soil particles, we centrifuged the filtrate at 1753 rpm for 10 minutes, after which we
352 retained the supernatant containing suspended bacterial cells.

353 To enrich for predatory bacteria in the soil sample supernatant, we used *Pseudomonas* sp.
354 NC02 as prey, because it was also isolated from a soil environment (41). We cultured
355 *Pseudomonas* sp. NC02 overnight in 120 ml tryptic soy broth (TSB) at 28°C and 200 rpm, then
356 centrifuged the culture at 6000 rpm for 10 minutes, washed the resulting pellet with 100 ml
357 sterile HM buffer, centrifuged again and resuspended the resulting pellet in 2.5 ml HM buffer.
358 We combined 1 ml of *Pseudomonas* sp. NC02 resuspension with 20 ml of soil sample
359 supernatant and incubated this enrichment at 28°C and 200 rpm.
360 Once we observed small, fast-moving cells under 1000x phase-contrast microscopy, we
361 filtered the enrichment using a 0.45 μm filter and performed 10-fold serial dilutions of the filtrate
362 in sterile HM buffer. Dilutions were then plated using a double agar overlay method. For each
363 dilution of the filtrate to be plated, we combined 100 μl of the dilution, 250 μl of *Pseudomonas*
364 sp. NC02 at 10^8 cfu/ml and 4.5 ml of molten HM top agar (0.6% agar). After vortexing, we
365 poured this mixture onto HM agar plates (1.5% agar). We allowed the top agar to solidify at
366 room temperature, then incubated plates at 28°C until we observed plaques in the lawn of
367 *Pseudomonas* sp. NC02. To begin the process of obtaining a pure isolate, we used a sterile
368 Pasteur pipette to extract single, well-defined plaques from the top agar. We combined each
369 plaque with 500 μl of sterile HM buffer, incubated the plaque suspension at room temperature
370 for at least 5 minutes, then vortexed it vigorously.
371 To culture predatory bacteria from the plaque suspensions, we made lysates combining
372 300 μl of each plaque suspension, 1.5 ml of an overnight culture of *Serratia* 0043 and 20 ml
373 sterile HM buffer. *Serratia* 0043 was also isolated from a soil environment, and switching to this
374 prey species during the isolation procedure selected for predatory isolates that were capable of
375 attacking multiple different soil bacteria. We incubated lysates at 28°C and 200 rpm. After 48 h,

376 one lysate showed small, fast-moving cells, and we used this lysate to begin two additional
377 rounds of serial dilution, plating and plaque picking to ensure a pure isolate. We used *Serratia*
378 0043 as prey during both of these rounds. After the final round, we filtered the plaque suspension
379 using a 0.45 μm filter, then combined 500 μl of filtrate with 500 μl of sterile 50% glycerol and
380 stored the stock at -80°C.

381 To classify NC01, we extracted the 16S rRNA gene sequence from the NC01 genome
382 based on the annotation generated by PGAP (see below for genome sequencing and annotation
383 methods). Using SINA 1.2.11 (39), we aligned this sequence against 16S rRNA gene sequences
384 from all nine delta-proteobacterial obligate predatory bacteria with complete genomes available
385 in GenBank at the time (*Bacteriovorax stolpii* DSM12778 CP025704, *Bdellovibrio*
386 *bacteriovorus* 109J CP007656, *Bdellovibrio bacteriovorus* HD100 NC_005363, *Bdellovibrio*
387 *bacteriovorus* SSB218315 CP020946, *Bdellovibrio bacteriovorus* Tiberius NC_019567,
388 *Bdellovibrio bacteriovorus* W NZ_CP002190, *Bdellovibrio exovorus* JSS NC_020813,
389 *Halobacteriovorax marinus* BE01 CP017414, *Halobacteriovorax marinus* SJ NC_016620). We
390 then inferred a phylogeny from the alignment with the online server RAxML Blackbox (42),
391 using 100 bootstrap replicates to estimate the confidence of the topology.

392 To further investigate the relationships among NC01 and other *Bdellovibrio*, we used an
393 average amino acid identity (AAI) calculator (http://enve-omics.ce.gatech.edu/) (43) to analyze
394 the similarity among protein-coding sequences from NC01, 109J, HD100 and W, as annotated by
395 RAST (see below for genome sequencing and annotation methods).

396 **Negative stain electron microscopy of *Bdellovibrio* sp. NC01**

397 To obtain samples of *Bdellovibrio* sp. NC01 for negative stain electron microscopy, we
398 added a small amount of the -80°C freezer stock to HM buffer mixed with 1.5 ml of an overnight

399 culture of *E. coli* ML35. After 48 h of incubation at 28°C and 200 rpm, we stained samples with
400 uranyl acetate following a previously described procedure (24) and imaged the resulting
401 specimens using a JEOL CX 2000 transmission electron microscope.

402 **Genome sequencing, annotation and analysis of *Bdellovibrio* sp. NC01**

403 To obtain genomic DNA, we combined a small amount of the -80°C stock, 1.5 ml of an
404 overnight culture of *E. coli* ML35 and 25 ml of sterile HM buffer. We chose ML35 as prey
405 because the genome sequence is available for screening reads if needed (44). After 72 hours of
406 incubation at 28°C and 200 rpm, we centrifuged the lysate at 9100 rpm for 10 minutes to pellet
407 bacterial cells. Because PacBio sequencing technology requires at least 10 μg of genomic DNA,
408 we did not filter the lysate to prevent loss of predatory bacteria cells. We then used the Wizard
409 Genomic DNA purification kit to extract genomic DNA, following the manufacturer's
410 instructions beginning with resuspension of the pellet in 600 μl of the kit's nuclei lysis solution.
411 For the final rehydration step, we rehydrated the DNA pellet overnight at 4°C. Quantification by
412 Qubit estimated a final concentration of 340 ng/μl genomic DNA.

413 For long-read sequencing, library construction and sequencing were performed at the
414 Institute for Genome Sciences at the University of Maryland Baltimore on a Pacific Biosciences
415 RSII instrument using P6-C4 chemistry. Quality control analysis of the reads showed that <10%
416 of reads aligned by BLAST to *E. coli* or *Shigella*, indicating that representation of the prey
417 genome in the read dataset is low. To analyze and assemble the reads, we launched an instance
418 of SMRT Portal 2.3.0 using Amazon EC2. A single SMRT cell yielded 79,088 postfilter
419 polymerase reads (N_{50} 17,028) and 94,031 subreads (N_{50} 13,572). Within SMRT Portal, we
420 assembled the reads with HGAP3 (45), using 4.5 Mbp for the genome size. This generated 186
421 contigs. The largest contig was 4,001,137 bp and aligned to *Bdellovibrio* in the database using

422 BLASTN. The other 185 contigs were each <48,000 bp in length, and all of them aligned to *E.*
423 *coli* by BLASTN, which is expected due to the inclusion of prey genomic DNA in the
424 sequencing library.

425 To close the genome, we used BLASTN to identify overlap in the ends of the contig and
426 trimmed the sequence to generate a closed contig of 3,975,771. We also adjusted the start site so
427 that the first nucleotide of the closed genome sequence corresponds to the first nucleotide in the
428 start codon of *dnaA*. To polish this sequence, we used 250 bp paired-end Illumina MiSeq data
429 generated at the Rhode Island Genomics and Sequencing Center. We filtered and trimmed the
430 raw read dataset to retain only those read pairs for which the quality score of every base was ≥13
431 and the read length was ≥65. This yielded 1,256,135 read pairs. Using bwa-mem (46), samtools
432 (47) and Pilon (48), we aligned these reads to the closed genome sequence and corrected 1 SNP,
433 84 small insertions totaling 85 bases and 4 small single-base deletions. We manually examined
434 changes flagged by Pilon using the alignment viewer Tablet (49), generating a final, polished
435 *Bdellovibrio* sp. NC01 genome sequence of 3,975,853 bp. This sequence has been deposited in
436 GenBank as CP030034.

437 In addition to annotation with NCBI's Prokaryotic Genome Annotation Pipeline (PGAP)
438 version 4.5, we also annotated the sequence using ClassicRAST (50, 51), Infernal (52), and
439 tRNAScan-SE (53, 54). For genome-wide pairwise comparisons, we used the BLAST Ring
440 Image Generator (BRIG) (55).

441 **Phenotype assays to test prey range and predation efficiency**

442 We obtained *Bdellovibrio bacteriovorus* HD100 from Mark Martin (University of Puget
443 Sound, Puget Sound, WA) for predatory phenotype comparisons. To culture *Bdellovibrio* NC01
444 and HD100, we added a small amount of -80°C stocks to 20 ml HM buffer combined with 1.5 ml

445 of an overnight culture of *E. coli* ML35. After 72 hours of incubation at 28°C and 200 rpm, we
446 filtered the lysate using a 0.45 μm filter to separate predatory cells from prey cells and cell debris.
447 For each phenotype assay described below, we followed this protocol to obtain attack phase
448 *Bdellovibrio* cells.

449 To test prey range and plaque appearance, we plated 10-fold serial dilutions of filtered
450 lysate using a double agar overlay method as described above for the isolation procedure. Each
451 tested prey strain was grown in 120 ml TSB overnight at 28°C and 200 rpm, with the exception
452 of *Escherichia* strains, which were grown at 37°C. After centrifugation and washing, we
453 resuspended prey cell pellets in 5 ml of sterile HM buffer. Based on cfu/ml counts, this yielded
454 concentrations of at least 10^8 cfu/ml, which ensured a dense prey lawn for visualizing plaques.
455 For some prey strains, we added 500 μl of prey resuspension to top agar to improve our ability to
456 detect and observe plaques in the prey lawn. We incubated plates at 28°C for 8 days before
457 scoring plaque formation and performed three replicates for each prey strain. In observations of
458 plaque appearance, we photographed plates at multiple time points over the course of 8 days.

459 To test predation efficiency, we adapted a protocol described in (15). We centrifuged the
460 filtered lysate at 8500 rpm for 10 minutes. The resulting pellet of predatory bacteria was
461 resuspended in sterile HM buffer to yield ~10^8 cells/ml based on direct cell counts using a
462 Petroff-Hausser counting chamber. To ensure that direct cell counts provided accurate estimates
463 of active predatory bacteria concentrations, we validated the method by comparing cells/ml
464 estimated using the Petroff-Hausser counting chamber with plaque-forming units/ml estimated
465 using serial dilution and double agar overlay to count plaques in a prey lawn. Results from two
466 replicates showed that direct cell counts were slightly lower than pfu/ml counts, but within the

467 same order of magnitude (direct cell counts: 3.94 x 10^8 cells/ml and 2.58 x 10^8 cells/ml, plaque
468 counts: 9.2 x 10^8 pfu/ml and 4.7 x 10^8 cells/ml).

469 To initiate the predation efficiency assay, we combined 500 µl of *Bdellovibrio* cell
470 resuspension (at ~10^8 cells/ml) with 12.5 ml of an overnight culture of *E. coli* ML35 diluted to
471 OD_{600} 0.15 (range: 0.135 – 0.165). This yielded ~10^8 cfu/ml, therefore the predation efficiency
472 assay results reported here are based on a predator:prey ratio of approximately 1:1. As a control,
473 we used 500 µl of sterile HM buffer in place of *Bdellovibrio* cell resuspension. Using cfu/ml
474 counts, we quantified viable *E. coli* ML35 at the beginning of the assay (time zero) and then after
475 6, 24, 48 and 72 hours of incubation at 28°C and 200 rpm.

476 **Acknowledgements**

477 This research was supported by an Institutional Development Award (IDeA) from the
478 National Institute of General Medical Sciences of the National Institutes of Health under grant no.
479 P20GM103430 and by funding from Providence College. This material is based upon work
480 conducted at a Rhode Island NSF EPSCoR research facility, the Genomics and Sequencing
481 Center, supported in part by the National Science Foundation EPSCoR Cooperative Agreement
482 #EPS-1004057. This material is based upon work supported in part by the National Science
483 Foundation under EPSCoR Cooperative Agreement #OIA-1655221. The funders had no role in
484 study design, data collection and interpretation, or the decision to submit the work for
485 publication.

486 We thank Lisa Sadzewicz and Luke Tallon at the Institute for Genome Sciences at the
487 University of Maryland Baltimore for PacBio sequencing services. We thank Janet Atoyan at the
488 Rhode Island Genomics and Sequencing Center for Illumina MiSeq sequencing services. We

489 thank Sean O'Donnell for isolating freshwater prey bacteria and Mark Martin and Brett Pellock
490 for donating bacterial strains.

491 **References**

492 1. Jurkevitch E, Davidov Y. 2007. Phylogenetic diversity and evolution of predatory
493 prokaryotes, p. 11–56. *In* Jurkevitch, E (ed.), Predatory Prokaryotes: Biology, Ecology and
494 Evolution. Springer Berlin Heidelberg, Berlin, Heidelberg.

495 2. Chen H, Laws EA, Martin JL, Berhane T-K, Gulig PA, Williams HN. 2018. Relative
496 contributions of *Halobacteriovorax* and bacteriophage to bacterial cell death under various
497 environmental conditions. MBio 9.

498 3. Welsh RM, Zaneveld JR, Rosales SM, Payet JP, Burkepile DE, Thurber RV. 2016.
499 Bacterial predation in a marine host-associated microbiome. ISME J 10:1540–1544.

500 4. Feng S, Tan CH, Constancias F, Kohli GS, Cohen Y, Rice SA. 2017. Predation by
501 *Bdellovibrio bacteriovorus* significantly reduces viability and alters the microbial
502 community composition of activated sludge flocs and granules. FEMS Microbiol Ecol 93.

503 5. Dwidar M, Monnappa AK, Mitchell RJ. 2012. The dual probiotic and antibiotic nature of
504 *Bdellovibrio bacteriovorus*. BMB Rep 45:71–78.

505 6. Kadouri DE, To K, Shanks RMQ, Doi Y. 2013. Predatory bacteria: a potential ally against
506 multidrug-resistant Gram-negative pathogens. PLoS ONE 8:e63397.

507 7. Tyson J, Sockett RE. 2017. Nature knows best: employing whole microbial strategies to
508 tackle antibiotic resistant pathogens. Environmental Microbiology Reports 9:47–49.

509 8. Martin MO. 2002. Predatory prokaryotes: an emerging research opportunity. J Mol
510 Microbiol Biotechnol 4:467–477.

511 9. Koval SF, Hynes SH, Flannagan RS, Pasternak Z, Davidov Y, Jurkevitch E. 2013.
512 *Bdellovibrio exovorus* sp. nov., a novel predator of *Caulobacter crescentus*. Int J Syst Evol
513 Microbiol 63:146–151.

514 10. Sockett RE. 2009. Predatory lifestyle of *Bdellovibrio bacteriovorus*. Annu Rev Microbiol
515 63:523–539.

516 11. Kuru E, Lambert C, Rittichier J, Till R, Ducret A, Derouaux A, Gray J, Biboy J, Vollmer W,
517 VanNieuwenhze M, Brun YV, Sockett RE. 2017. Fluorescent D-amino-acids reveal bi-
518 cellular cell wall modifications important for *Bdellovibrio bacteriovorus* predation. Nat
519 Microbiol 2:1648–1657.

520 12. Lerner TR, Lovering AL, Bui NK, Uchida K, Aizawa S-I, Vollmer W, Sockett RE. 2012.
521 Specialized peptidoglycan hydrolases sculpt the intra-bacterial niche of predatory
522 *Bdellovibrio* and increase population fitness. PLOS Pathogens 8:e1002524.

523 13. Dashiff A, Junka RA, Libera M, Kadouri DE. 2011. Predation of human pathogens by the
524 predatory bacteria *Micavibrio aeruginosavorus* and *Bdellovibrio bacteriovorus*. Journal of
525 Applied Microbiology 110:431–444.

526 14. Jurkevitch E, Minz D, Ramati B, Barel G. 2000. Prey range characterization, ribotyping,
527 and diversity of soil and rhizosphere *Bdellovibrio* spp. isolated on phytopathogenic bacteria.
528 Appl Environ Microbiol 66:2365–2371.

529 15. Rogosky AM, Moak PL, Emmert EAB. 2006. Differential predation by *Bdellovibrio*
530 *bacteriovorus* 109J. Curr Microbiol 52:81–85.

531 16. Rendulic S, Jagtap P, Rosinus A, Eppinger M, Baar C, Lanz C, Keller H, Lambert C, Evans
532 KJ, Goesmann A, Meyer F, Sockett RE, Schuster SC. 2004. A predator unmasked: life
533 cycle of *Bdellovibrio bacteriovorus* from a genomic perspective. Science 303:689–692.

534 17. Negus D, Moore C, Baker M, Raghunathan D, Tyson J, Sockett RE. 2017. Predator versus
535 pathogen: How does predatory *Bdellovibrio bacteriovorus* interface with the challenges of
536 killing Gram-negative pathogens in a host setting? Annu Rev Microbiol 71:441–457.

537 18. Hoeniger JFM, Ladwig R, Moor H. 1972. The fine structure of "resting bodies" of
538 *Bdellovibrio* sp. strain W developed in *Rhodospirillum rubrum*. Can J Microbiol 18:87–92.

539 19. Oyedara OO, Segura-Cabrera A, Guo X, Elufisan TO, Cantú González RA, Rodríguez
540 Pérez MA. 2018. Whole-genome sequencing and comparative genome analysis provided
541 insight into the predatory features and genetic diversity of two *Bdellovibrio* species isolated
542 from soil. Int J Genomics 2018.

543 20. Stackebrandt E, Goebel BM. 1994. Taxonomic note: A place for DNA-DNA reassociation
544 and 16S rRNA sequence analysis in the present species definition in bacteriology.
545 International Journal of Systematic and Evolutionary Microbiology 44:846–849.

546 21. Stackebrandt E, Ebers J. 2006. Taxonomic parameters revisited: tarnished gold standards.
547 Microbiology Today 33:152–155.

548 22. Ravenhall M, Škunca N, Lassalle F, Dessimoz C. 2015. Inferring horizontal gene transfer.
549 PLoS Comput Biol 11.

550 23. Tudor JJ, Conti SF. 1977. Characterization of bdellocysts of *Bdellovibrio* sp. Journal of
551 Bacteriology 131:314–322.

552 24. Enos BG, Anthony MK, DeGiorgis JA, Williams LE. 2018. Prey range and genome
553 evolution of *Halobacteriovorax marinus* predatory bacteria from an estuary. mSphere
554 3:e00508-17.

555 25. Gophna U, Charlebois RL, Doolittle WF. 2006. Ancient lateral gene transfer in the
556 evolution of *Bdellovibrio bacteriovorus*. Trends Microbiol 14:64–69.

557 26. Pan A, Chanda I, Chakrabarti J. 2011. Analysis of the genome and proteome composition
558 of *Bdellovibrio bacteriovorus*: indication for recent prey-derived horizontal gene transfer.
559 Genomics 98:213–222.

560 27. Hobley L, Lerner TR, Williams LE, Lambert C, Till R, Milner DS, Basford SM, Capeness
561 MJ, Fenton AK, Atterbury RJ, Harris MATS, Sockett RE. 2012. Genome analysis of a
562 simultaneously predatory and prey-independent, novel *Bdellovibrio bacteriovorus* from the
563 River Tiber, supports in silico predictions of both ancient and recent lateral gene transfer
564 from diverse bacteria. BMC Genomics 13:670.

565 28. Fratamico PM, Whiting RC. 1995. Ability of *Bdellovibrio bacteriovorus* 109J to lyse
566 Gram-negative food-borne pathogenic and spoilage bacteria. Journal of Food Protection
567 58:160–164.

568 29. Baker M, Negus D, Raghunathan D, Radford P, Moore C, Clark G, Diggle M, Tyson J,
569 Twycross J, Sockett RE. 2017. Measuring and modelling the response of *Klebsiella*
570 *pneumoniae* KPC prey to *Bdellovibrio bacteriovorus* predation, in human serum and
571 defined buffer. Sci Rep 7:8329.

572 30. Shemesh Y, Jurkevitch E. 2004. Plastic phenotypic resistance to predation by *Bdellovibrio*
573 and like organisms in bacterial prey. Environ Microbiol 6:12–18.

574 31. Cotter TW, Thomashow MF. 1992. Identification of a *Bdellovibrio bacteriovorus* genetic
575 locus, *hit*, associated with the host-independent phenotype. J Bacteriol 174:6018–6024.

576 32. Roschanski N, Klages S, Reinhardt R, Linscheid M, Strauch E. 2011. Identification of
577 genes essential for prey-independent growth of *Bdellovibrio bacteriovorus* HD100. Journal
578 of Bacteriology 193:1745–1756.

579 33. Marchesi JR, Sato T, Weightman AJ, Martin TA, Fry JC, Hiom SJ, Dymock D, Wade WG.
580 1998. Design and evaluation of useful bacterium-specific PCR primers that amplify genes
581 coding for bacterial 16S rRNA. Appl Environ Microbiol 64:795–799.

582 34. Heuer H, Krsek M, Baker P, Smalla K, Wellington EM. 1997. Analysis of actinomycete
583 communities by specific amplification of genes encoding 16S rRNA and gel-electrophoretic
584 separation in denaturing gradients. Appl Environ Microbiol 63:3233–3241.

585 35. Ewing B, Green P. 1998. Base-calling of automated sequencer traces using Phred. II. Error
586 probabilities. Genome Res 8:186–194.

587 36. Ewing B, Hillier L, Wendl MC, Green P. 1998. Base-calling of automated sequencer traces
588 using Phred. I. Accuracy assessment. Genome Res 8:175–185.

589 37. Gordon D, Abajian C, Green P. 1998. Consed: A graphical tool for sequence finishing.
590 Genome Res 8:195–202.

591 38. Altschul SF, Gish W, Miller W, Myers EW, Lipman DJ. 1990. Basic local alignment search
592 tool. Journal of Molecular Biology 215:403–410.

593 39. Pruesse E, Peplies J, Glöckner FO. 2012. SINA: Accurate high-throughput multiple
594 sequence alignment of ribosomal RNA genes. Bioinformatics 28:1823–1829.

595 40. Wang Q, Garrity GM, Tiedje JM, Cole JR. 2007. Naïve Bayesian classifier for rapid
596 assignment of rRNA sequences into the new bacterial taxonomy. Appl Environ Microbiol
597 73:5261–5267.

598 41. Cerra J, Donohue H, Kral A, Oser M, Rostkowski L, Zappia L, Williams LE. 2018.
599 Complete genome sequence of *Pseudomonas* sp. strain NC02, isolated from soil. Genome
600 Announc 6.

601 42. Kozlov A, Darriba D, Flouri T, Morel B, Stamatakis A. 2018. RAxML-NG: A fast, scalable,
602 and user-friendly tool for maximum likelihood phylogenetic inference. bioRxiv 447110.

603 43. Rodriguez-R LM, Konstantinidis KT. 2016. The enveomics collection: a toolbox for
604 specialized analyses of microbial genomes and metagenomes. PeerJ Preprints 4:e1900v1.

605 44. Casale A, Clark S, Grasso M, Kryschuk M, Ritzer L, Trudeau M, Williams LE. 2018.
606 Complete genome sequence of *Escherichia coli* ML35. Genome Announc 6.

607 45. Chin C-S, Alexander DH, Marks P, Klammer AA, Drake J, Heiner C, Clum A, Copeland A,
608 Huddleston J, Eichler EE, Turner SW, Korlach J. 2013. Nonhybrid, finished microbial
609 genome assemblies from long-read SMRT sequencing data. Nature Methods 10:563–569.

610 46. Li H, Durbin R. 2009. Fast and accurate short read alignment with Burrows–Wheeler
611 transform. Bioinformatics 25:1754–1760.

612 47. Li H, Handsaker B, Wysoker A, Fennell T, Ruan J, Homer N, Marth G, Abecasis G, Durbin
613 R. 2009. The Sequence Alignment/Map format and SAMtools. Bioinformatics 25:2078–
614 2079.

615 48. Walker BJ, Abeel T, Shea T, Priest M, Abouelliel A, Sakthikumar S, Cuomo CA, Zeng Q,
616 Wortman J, Young SK, Earl AM. 2014. Pilon: An integrated tool for comprehensive
617 microbial variant detection and genome assembly improvement. PLOS ONE 9:e112963.

618 49. Milne I, Stephen G, Bayer M, Cock PJA, Pritchard L, Cardle L, Shaw PD, Marshall D.
619 2013. Using Tablet for visual exploration of second-generation sequencing data. Brief
620 Bioinform 14:193–202.

621 50. Aziz RK, Bartels D, Best AA, DeJongh M, Disz T, Edwards RA, Formsma K, Gerdes S,
622 Glass EM, Kubal M, Meyer F, Olsen GJ, Olson R, Osterman AL, Overbeek RA, McNeil
623 LK, Paarmann D, Paczian T, Parrello B, Pusch GD, Reich C, Stevens R, Vassieva O,
624 Vonstein V, Wilke A, Zagnitko O. 2008. The RAST Server: rapid annotations using
625 subsystems technology. BMC Genomics 9:75.

626 51. Overbeek R, Olson R, Pusch GD, Olsen GJ, Davis JJ, Disz T, Edwards RA, Gerdes S,
627 Parrello B, Shukla M, Vonstein V, Wattam AR, Xia F, Stevens R. 2014. The SEED and the

628 Rapid Annotation of microbial genomes using Subsystems Technology (RAST). Nucleic
629 Acids Res 42:D206-214.

630 52. Nawrocki EP, Eddy SR. 2013. Infernal 1.1: 100-fold faster RNA homology searches.
631 Bioinformatics 29:2933–2935.

632 53. Lowe TM, Chan PP. 2016. tRNAscan-SE On-line: integrating search and context for
633 analysis of transfer RNA genes. Nucleic Acids Res 44:W54-57.

634 54. Lowe TM, Eddy SR. 1997. tRNAscan-SE: a program for improved detection of transfer
635 RNA genes in genomic sequence. Nucleic Acids Res 25:955–964.

636 55. Alikhan N-F, Petty NK, Ben Zakour NL, Beatson SA. 2011. BLAST Ring Image Generator
637 (BRIG): simple prokaryote genome comparisons. BMC Genomics 12:402.

638 **Figures and Figure Legends**

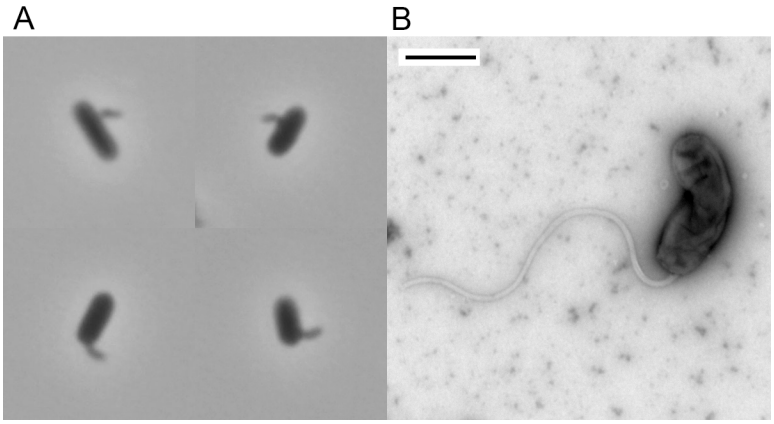

639

640 **Figure 1.** Microscopy of *Bdellovibrio* sp. NC01 isolated from bioswale soil. (A) Compilation of
641 four images taken using 1000x phase-contrast microscopy to show small, comma-shaped NC01
642 attack phase cells attached to larger *E. coli* ML35 cells after 48 hours of co-culture. (B) Negative
643 stain electron microscopy of a NC01 attack phase cell. The scale bar is 500 nm.

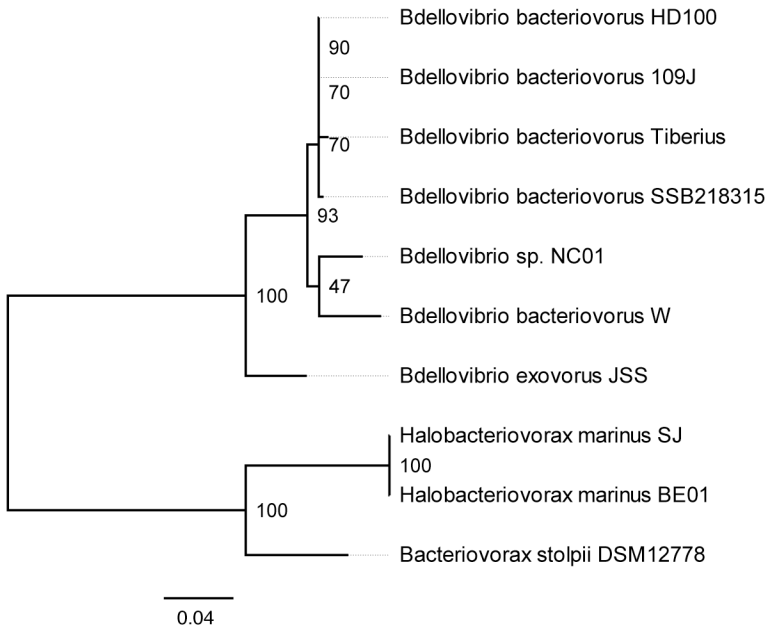

Figure 2. 16S rRNA gene phylogeny. We aligned 16S rRNA gene sequences using SINA 1.2.11, then constructed a phylogeny using RAxML BlackBox with 100 bootstrap replicates. The phylogeny is rooted on the branch joining *Bdellovibrio* with *Bacteriovorax*/*Halobacteriovorax*, and bootstrap support for each node is shown.

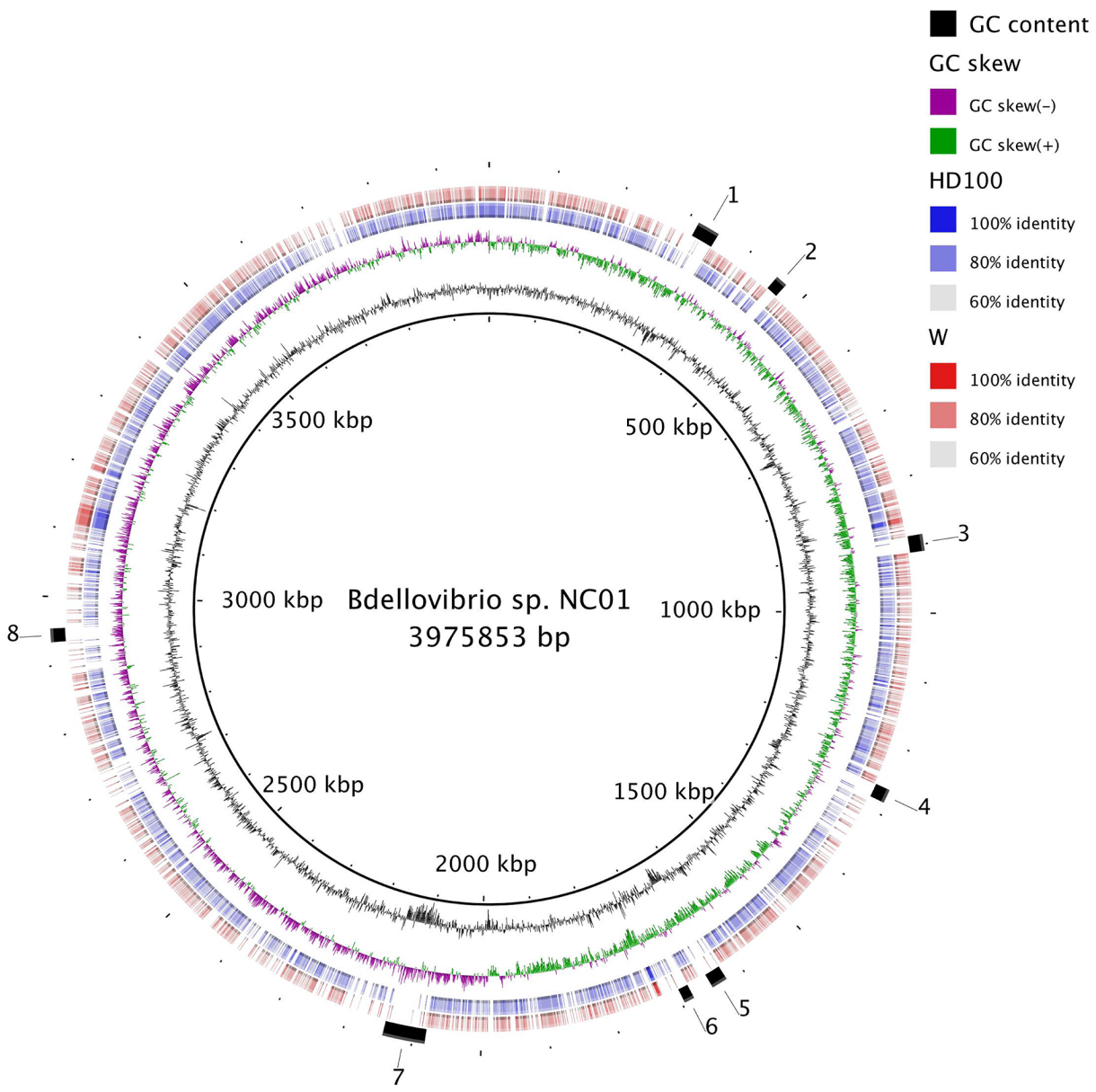

Figure 3. Genome-wide pairwise comparisons of *Bdellovibrio* nucleotide sequences. The genome of *Bdellovibrio* sp. NC01 is shown as the innermost ring. The next ring is a plot of GC content and the purple and green ring is a plot of GC skew, both of which were generated by the BLAST Ring Image Generator (BRIG) using sliding windows to determine deviation from the average value for the genome. The blue ring and red ring show pairwise nucleotide sequence alignments of NC01 to HD100 and W, respectively. Each individual alignment is shown as a block along the ring, and color gradation of the blocks reflects the percent similarity of

657 alignments. The outermost ring denotes eight regions lacking alignments, which may indicate

658 unique NC01 gene content.

659

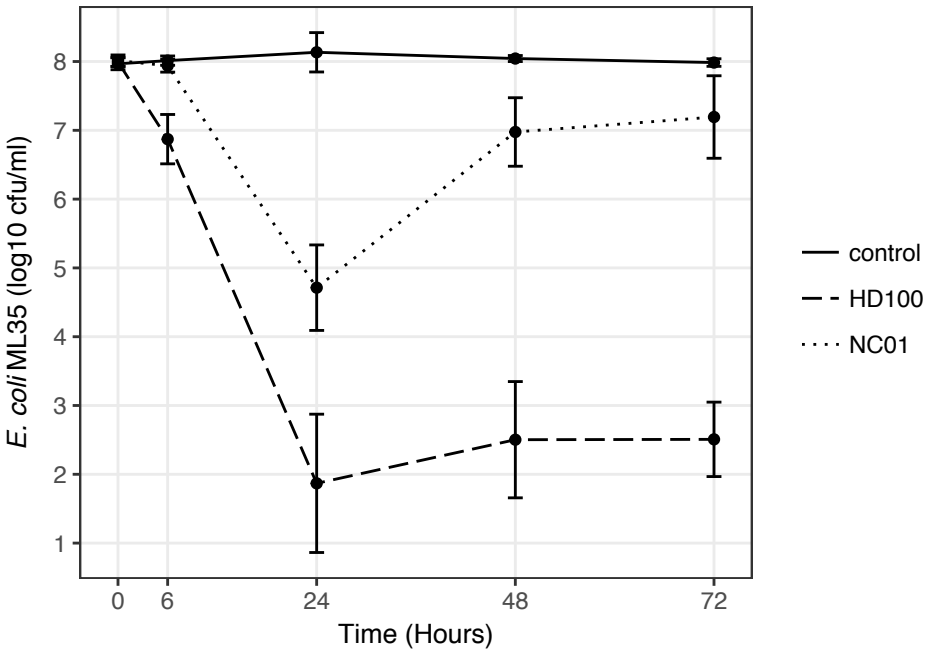

660

661 **Figure 4.** Efficiency of *Bdellovibrio* sp. NC01 and *B. bacteriovorus* HD100 predation on *E. coli*

662 ML35. We quantified viable *E. coli* ML35 over 72 hours on its own (control), combined with

663 *Bdellovibrio* sp. NC01 (NC01) and combined with *B. bacteriovorus* HD100 (HD100). The

664 resulting cfu/ml data were log transformed and plotted using ggplot in RStudio. Each time point

665 shows the mean and standard deviation for at least five replicates.

666

667 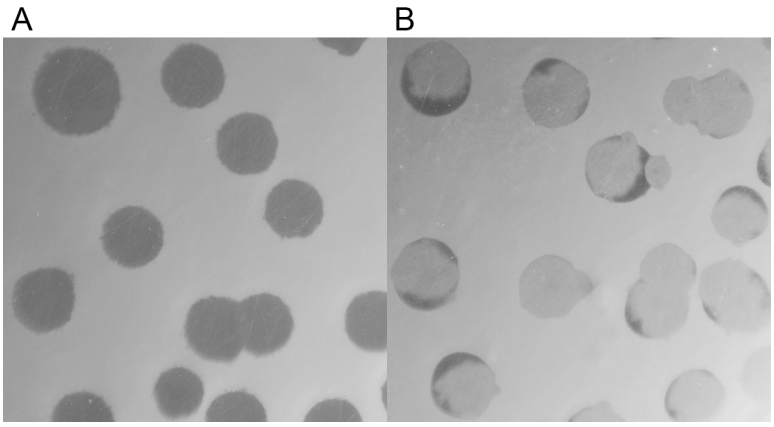

668 **Figure 5.** Plaque phenotypes of *Bdellovibrio* sp. NC01 and *B. bacteriovorus* HD100. Using a
669 double agar overlay method, we assessed plaque formation on lawns of *E. coli* ML35. These
670 images were taken after 6 days of incubation and illustrate reproducible differences in the
671 appearance of plaques formed by HD100 (A) and NC01 (B).
672

673 **Tables**

674 Table 1. Average amino acid identity among *Bdellovibrio* genomes

	NC01	W	HD100	109J
NC01		64.4	68.8	68.8
W	64.4		66.4	66.5
HD100	68.8	66.4		99.2
109J	68.8	66.5	99.2	

675

676 Table 2. Genome comparison of *Bdellovibrio* sp. NC01, *Bdellovibrio bacteriovorus* HD100 and
677 *Bdellovibrio bacteriovorus* W
678

	Bdellovibrio sp. NC01		*Bdellovibrio bacteriovorus* HD100		*Bdellovibrio bacteriovorus* W	
	PGAP	RAST and RFAM/ tRNAScan	PGAP	RAST and RFAM/ tRNAScan	PGAP	RAST and RFAM/ tRNAScan
Genome size (bp)	3,975,853		3,782,950		3,006,992	
GC content (%)	44.5		50.6		43.3	
Genes	3,840	3,828	3,597	3,651	2,834	2,901
Protein-coding	3,773	3,776	3,548	3,597	2,760	2,849
Hypothetical proteins	1,712	1,431	1,245	1,309	962	971
tRNA	34	34	36	36	34	34
rRNA	6	6	6	6	6	6
Other RNA	4	12	4	12	4	12

679

680 Table 3. Prey range of *B. bacteriovorus* HD100 and *Bdellovibrio* sp. NC01

Genus	Strain ID	Environment	Plaque formation[a]	
			HD100	NC01
Acinetobacter	0036	Freshwater	Yes	No
Aeromonas	0031	Freshwater	Yes	Yes
Enterobacteriaceae	0032	Freshwater	Yes	Yes
Raoultella	0037	Freshwater	Yes	No
Pseudomonas	NC02 (0042)[b]	Soil	Yes	Yes
Serratia	0043	Soil	Yes	Yes
Escherichia	0057		Yes	No
Escherichia	ML35		Yes	Yes

681 [a]Plaque formation data based on three replicates

682 [b]*Pseudomonas* sp. NC02 is referred to as 0042 in (27)

683